



Cover Page



SYNTHESIS AND LUMINESCENCE STUDY OF FLUORINATED AROMATIC ACID AND BIDENTATE (N-DONOR) ANCILLARY LIGANDS BASED EUROPIUM COMPLEXES FOR ADVANCED OPTOELECTRONIC DEVICES AND BIOLOGICAL QUANTIFICATION

Jyoti Khanagwal

Rajiv Gandhi Govt. College for Women, Bhiwani, India

Abstract

A new family of five europium(III) cored complexes has been fabricated via a cost effective solution precipitation approach with the utilization of 3-(1,1,2,2-tetrafluoroethoxy)benzoic acid (L) main ligand and ancillary ligands such as bathophenanthroline, 5,6-dimethyl-1,10-phenanthroline, 1,10-phenanthroline and 2,2-bipyridyl. The techniques of CHN and EDAX analyses detect the qualitative and quantitative compositions of ligand and complexes. $^1\text{H-NMR}$ and FT-IR spectral study confirms the binding modes of ligands in complexation with Eu^{3+} ion. The characterization regarding evaluation of band-gap energy values (3.91-3.37 eV) for complexes has been done by scanning diffuse reflectance spectra and values lie in range of wide band-gap semiconductors, thus it unveils the utility of these complexes in military sectors and laser diodes. By utilization of band-gap value, the refractive index of complexes (1.88-1.97) is determined. The optimum thermal stability of complexes indicates the applications of these complexes in fabrication of white light emitting diodes. The photoluminescence results justify the intense red emission of europium complexes as a consequence of $^5\text{D}_0 \rightarrow ^7\text{F}_2$ transition and existence of single emissive species is corroborated by evaluation of decay curves. The color purity (67.64-94.94 %) and color coordinates authenticates the monochromatic (red) emission of complexes. The greater sensitization effect of ligand is indicated by energy transfer mechanism. The antimicrobial (tube dilution method) and antioxidant potential (DPPH method) of complexes validates that the complexes possess good antimicrobial and antioxidant capacity. The investigated results expand the role of these luminescent complexes in photonic devices and luminescent solar concentrators (LSCs) based solar cells.

Keywords: Photoluminescence, Antioxidant features, Band-gap analysis, Quantum efficiency, Judd-Ofelt Intensity parameter, Photonic devices.

1. Introduction

The last few decades long, luminescent lanthanide complexes have become the centre of attention for the research community in the view of their most promising applications such as lighting devices, sensors [1], optical amplifiers [2], lasers, enzyme activity assay [3], luminescent solar concentrators [4] and bioimaging [5]. The fascinating emission spectral characteristics such as high color purity, large value of stokes shift, long ranged emission lifetime and sharp emission bands of lanthanide ions make them the point of convergence for material society. Recently, with the development of society, the research on lanthanide luminescent materials has bloomed constantly. Although, the direct excitation of lanthanide ions normally favor low light absorbing capacity on account of parity forbidden nature of f-f transitions, which declines the luminescence performance of these ions [6]. Therefore, the enhanced luminescence performance of trivalent lanthanide ions can be achieved by linkage of light harvesting organic ligands with metal ion, which boosts the luminescence efficiency via antenna effect [7]. In addition, extended π -conjugated antennae molecules as chromophores are useful in flexible and light weight optical devices, white organic light emitting diodes (WOLEDs), hence, the researchers and material scientists are engaged in investigation and synthesis of such types of chromophores (organic ligands) [8]. The fluorinated aromatic carboxylic acid is recognized as an adequate antenna molecule which encourages the energy transfer process via quenching of non-radiatively energy loss occurs by vibration of C-H bonds. It is because of larger mass of C-F group as compared to its hydrogenated counterparts (C-H). The luminescence efficiency of organo lanthanide complexes can be further enhanced by introduction of second chromophores (ancillary ligands) in the coordination sphere of lanthanide complexes that ancillary ligands satisfy the coordination number of lanthanide ions as well as provide coordinatively rigid system and remove the vibronic quenching induced by water molecules existing in chelated framework of lanthanide complexes. Among lanthanide



Cover Page



ions, Eu^{3+} ion complexes are considered as promising candidate in display devices and laser system due to intense red emission arising from $^5\text{D}_0 \rightarrow ^7\text{F}_2$ electronic transition [9].

Thus by considering the above physiochemical properties, five luminescent Eu^{3+} ion based complexes of π -conjugated 3-(1,1,2,2-tetrafluoroethoxy)benzoic acid (L) as main organic ligand and different ancillary ligands like bathophenanthroline (batho), 5,6-dimethyl-1,10-phenanthroline (dmph), 1,10-phenanthroline (phen) and 2,2-bipyridyl (bipy) have been prepared through less time consuming solution precipitation approach. The elemental and structural information of complexes can be gained through elemental analysis, EDAX (energy dispersive X-ray analysis) and FT-IR (Fourier transform infrared), NMR (nuclear magnetic resonance) spectroscopy and TG/DTG (thermogravimetric and differential thermogravimetric) analysis, respectively. TG/DTG analysis is used to investigate the thermal stability whilst optical band-gap (E_g) determination is carried out by DR (diffuse reflectance) spectroscopy. The photoluminescence spectral records are performed to find out the optical properties of the complexes. SEM (scanning electron microscope) analysis identifies the morphology of particles (existing in the complexes). The antimicrobial and antioxidant investigations have been done successfully via tube dilution and 2,2-diphenyl-1-picrylhydrazyl (DPPH) approaches, respectively. Further, radiative and non-radiative decay constants and Judd-Ofelt intensity parameters have been enumerated from the emission spectral record. The process of energy transfer assesses the role of main ligand and ancillary ligands in sensitization of Eu^{3+} ion.

2. Experimental

2.1. Materials and methods

The chemicals and solvents utilized for synthesis of ligand (L) and complexes were of analytical grade and obtained from easily available source, Merck. All purchased chemicals and reagents were used without further purification.

The direct titration of EDTA (ethylenediaminetetraacetic acid) was used to evaluate the content of europium ion exhibited by the complexes. CHN 2400 elemental analyzer (Perkin Elmer) was used to record CHN (carbon, hydrogen, nitrogen) elemental microanalysis and EDAX analysis were performed on Ametek EDAX. FT-IR spectra were measured in frequency span of $4000\text{--}400\text{ cm}^{-1}$ by using Perkin Elmer spectrum 400 FTIR/FT-FIR spectrophotometer with KBr pellet. $^1\text{H-NMR}$ spectra were scrutinized in CDCl_3 (deutrated chloroform) with the help of Bruker Avance II 400 NMR spectrometer. The absorption spectra in DMSO and solid DR spectra were carried out with Shimadzu UV-3600 Plus spectrophotometer. TG/DTG analysis was performed in the range of $32\text{--}850\text{ }^\circ\text{C}$ with the use of thermal analyzer (SDT Q600) in presence of inert atmosphere of nitrogen gas and $20\text{ }^\circ\text{C/min}$ heating rate. Hitachi F-7000 fluorescence spectrophotometer fitted with radiations source in the form of xenon lamp was employed to document the photoluminescence spectra. SEM analysis was done with the help of JEOL JSM-6510 and CIE color coordinates were evaluated by using MATLAB software.

2.2. Synthesis of ligand (L)

The eco-friendly method was applied for ligand synthetic process in which 3-hydroxybenzoate was produced by esterification reaction of 3-hydroxybenzoic acid in presence of methanol and H_2SO_4 (conc.). In second step, mixture of acetonitrile and 3-hydroxybenzoate was refluxed for about 48 h at $68\text{ }^\circ\text{C}$ followed by addition of K_2CO_3 and 1-bromo-1,1,2,2-tetrafluoroethane. The hydrolysis of obtained product was done with solution of KOH (aqueous) in ethanol and precipitations occur in solution with addition of dilute HCl solution. The purification of final crude with ethanol produced the pure product of 3-(1,1,2,2-tetrafluoroethoxy)benzoic acid (L) with 75 % yield [10]. IR (KBr): cm^{-1} 3009 (w), 2977 (w), 2928 (w), 2678 (w), 2569 (w), 2361 (w), 2344 (w), 1705 (s), 1685 (s), 1589 (s), 1534 (m), 1515 (s), 1424 (s), 1414 (m), 1383 (s), 1310 (s), 1274 (s), 1243 (s), 1206 (s), 1137 (m), 1115 (m), 1062 (m), 1037 (m), 995 (s), 960 (m), 948 (s), 900 (w), 851 (m), 822 (w), 794 (m), 783 (s), 754 (w), 745 (w), 698 (m), 677 (s), 596 (m), 548 (s), 474 (w), 434 (w); $^1\text{H-NMR}$ (CDCl_3 , 500 MHz): δ 5.80-6.08 (m, 1H, $-\text{CHF}_2$), 7.47-7.54 (m, 3H, Ar-H), 7.96 (s, 1H, Ar-H), 10.98 (s, 1H, $-\text{COOH}$) ppm. Anal. Cal. for $\text{C}_9\text{H}_6\text{O}_3\text{F}_4$: C, 45.39; H, 2.54; found: C, 45.38; H, 2.52.

2.3. Synthesis of europium complexes

The aqueous solution of $\text{Eu}(\text{NO}_3)_3 \cdot 5\text{H}_2\text{O}$ (1 mmol) was mixed constantly to the stirring ethanolic mixture of 3 mmol ligand (L) and pH ($\sim 6\text{--}7$) of stirring mixture was adjusted by addition of aqueous solution of NaOH in drops and stirred with proper heating. The binary complex C1 was recovered as off white precipitates. The liquid content of mixture was evaporated in an oven and obtained product was purified by washing thoroughly with ethanol. The precipitates of C1 complex were dried in oven at $45\text{ }^\circ\text{C}$.

The ternary complexes (C2-C5) were synthesized through similar synthetic operation in which mixture of aqueous solution of $\text{Eu}(\text{NO}_3)_3 \cdot 5\text{H}_2\text{O}$ and ethanolic solution of ligand L used in 1:3 molar ratio was mixed with 1 mmol ethanolic solution of



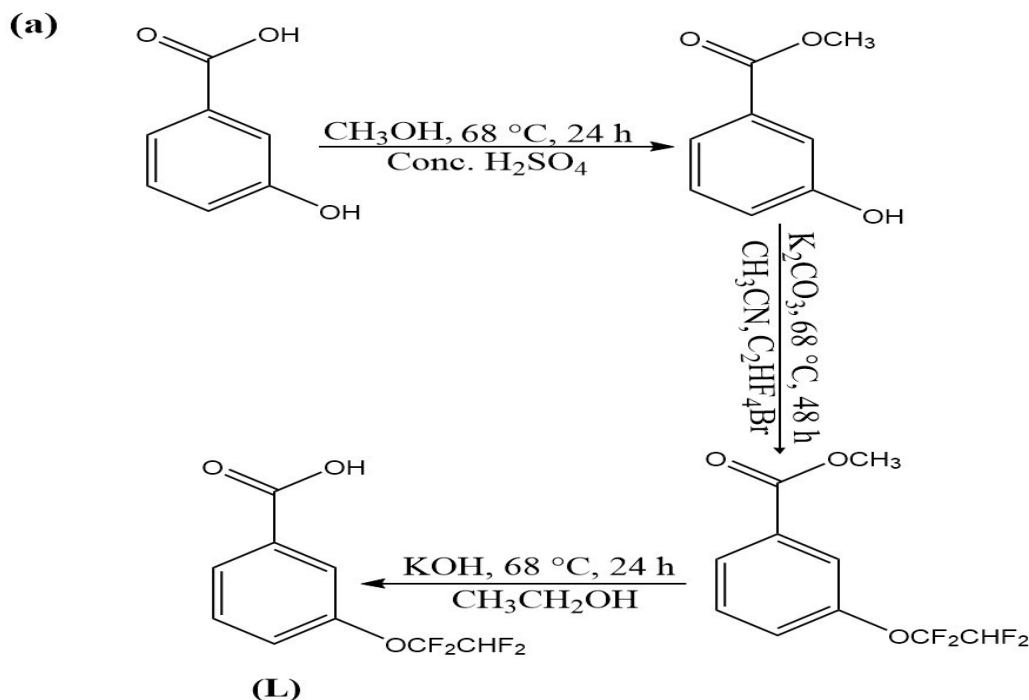
batho, dmph, phen and bipy ancillary ligands, respectively. For synthesis of $Gd(L)_3 \cdot 2H_2O$ (gadolinium complex of L), the aforementioned method (as employed for binary complex) was followed and this complex was utilized to assess the excited triplet (T_1) state of ligand (L). The synthetic procedure of ligand (L) and its related complexes of Eu^{3+} ion are manifested in **Scheme 1**.

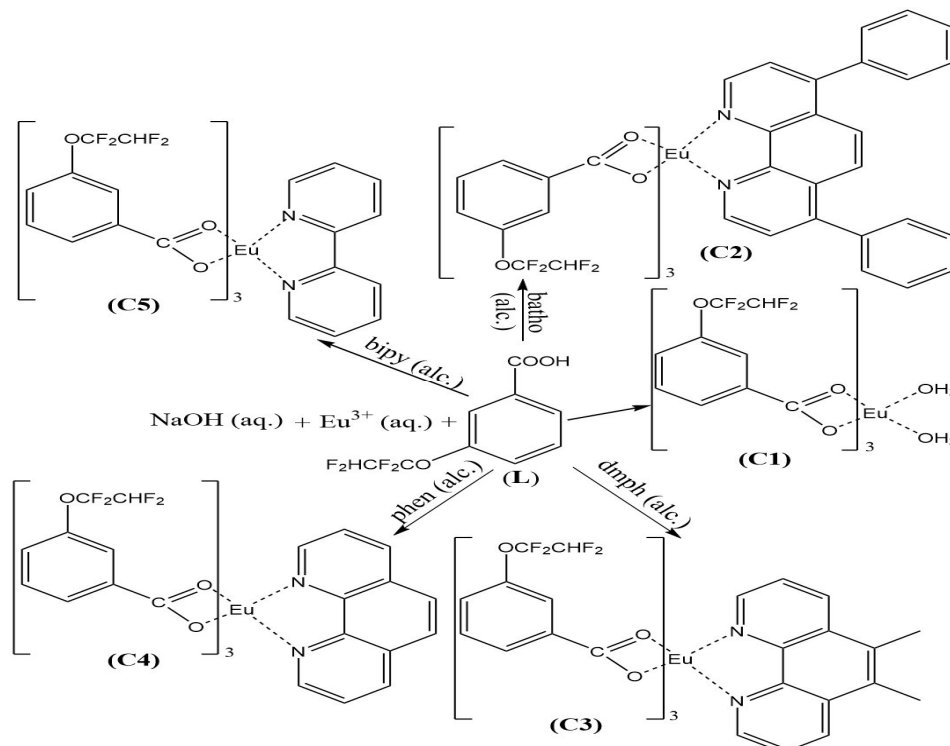
$Eu(L)_3 \cdot 2H_2O$ (C1): off white powder, yield 68 %. IR (KBr): cm^{-1} 3426 (b), 3079 (w), 3002 (w), 2430 (w), 1610 (s), 1573 (s), 1489 (w), 1443 (s), 1404 (s), 1303 (s), 1272 (s), 1205 (s), 1121 (s), 1003 (w), 955 (m), 932 (m), 852 (m), 837 (m), 791 (s), 768 (w), 747 (m), 681 (m), 596 (w), 552 (w), 522 (w), 425 (m); 1H -NMR ($CDCl_3$, 500 MHz): δ 1.92 (s, 4H, $-OH_2$), 2.18 (s, 3H, $-CHF_2$), 7.28 (m, 12H, Ar-H) ppm. Anal. Cal. for $EuC_{27}H_{19}O_{11}F_{12}$: C, 36.06; H, 2.13; Eu, 16.90; found: C, 36.09; H, 2.12; Eu, 16.88.

$Eu(L)_3 \cdot batho$ (C2): off white powder, yield 72 %. IR (KBr): cm^{-1} 3072 (w), 3002 (w), 2942 (w), 2433 (w), 2232 (w), 1633 (s), 1580 (s), 1566 (s), 1485 (w), 1441 (s), 1402 (s), 1302 (s), 1282 (s), 1201 (s), 1117 (s), 1003 (w), 954 (w), 926 (m), 844 (s), 791 (s), 762 (m), 747 (m), 682 (s), 635 (m), 599 (w), 571 (w), 545 (m), 522 (w), 420 (s); 1H -NMR ($CDCl_3$, 500 MHz): δ 5.35-5.62 (m, 3H, $-CHF_2$), 6.99 (s, 3H, Ar-H), 7.31-7.36 (d, 3H, Ar-H), 7.52-7.74 (d, 10H, Ar-H), 8.09-8.16 (d, 8H, Ar-H), 8.96-9.01 (d, 4H, Ar-H) ppm. Anal. Cal. for $EuC_{51}H_{31}N_2O_9F_{12}$: C, 51.23; H, 2.61; N, 2.34; Eu, 12.71; found: C, 51.22; H, 2.63; N, 2.35; Eu, 12.72.

$Eu(L)_3 \cdot dmph$ (C3): off white powder, yield 82 %. IR (KBr): cm^{-1} 3068 (w), 3001 (w), 2942 (w), 2428 (w), 2232 (w), 1635 (s), 1580 (s), 1544 (s), 1483 (w), 1439 (s), 1404 (s), 1301 (s), 1282 (s), 1197 (s), 1118 (s), 1003 (w), 952 (m), 928 (m), 848 (s), 788 (m), 765 (w), 746 (m), 683 (m), 638 (w), 598 (w), 573 (w), 545 (m), 518 (w), 423 (s); 1H -NMR ($CDCl_3$, 500 MHz): δ 5.34-5.61 (m, 3H, $-CHF_2$), 7.02 (s, 3H, Ar-H), 7.32-7.35 (d, 3H, Ar-H), 7.54-7.73 (d, 6H, Ar-H), 8.11-8.17 (d, 4H, Ar-H), 8.97-9.02 (d, 2H, Ar-H) ppm. Anal. Cal. for $EuC_{41}H_{27}N_2O_9F_{12}$: C, 45.95; H, 2.54; N, 2.61; Eu, 14.18; found: C, 45.97; H, 2.55; N, 2.59; Eu, 14.17.

$Eu(L)_3 \cdot phen$ (C4): off white powder, yield 78 %. IR (KBr): cm^{-1} 3067 (w), 3002 (w), 2941 (w), 2430 (w), 2232 (w), 1634 (s), 1580 (s), 1545 (s), 1485 (w), 1440 (s), 1403 (s), 1302 (s), 1282 (s), 1198 (s), 1117 (s), 1002 (w), 953 (m), 927 (m), 845 (s), 790 (m), 763 (w), 746 (m), 682 (m), 637 (w), 597 (w), 573 (w), 546 (m), 520 (w), 423 (s); 1H -NMR ($CDCl_3$, 500 MHz): δ 5.36-5.63 (m, 3H, $-CHF_2$), 7.00 (s, 3H, Ar-H), 7.36 (d, 6H, Ar-H), 7.52-7.75 (d, 5H, Ar-H), 8.13-8.18 (d, 4H, Ar-H), 8.99-9.03 (d, 2H, Ar-H) ppm. Anal. Cal. for $EuC_{39}H_{23}N_2O_9F_{12}$: C, 44.89; H, 2.22; N, 2.68; Eu, 14.56; found: C, 44.89; H, 2.21; N, 2.69; Eu, 14.56.





Scheme 1 Reaction mechanism for synthesis of L ligand (a) and complexes of trivalent europium ion (b).

Eu(L)₃.bipy (C5): off white powder, yield 85 %. IR (KBr): cm⁻¹ 3067 (w), 3001 (w), 2942 (w), 2432 (w), 1633 (s), 1581 (s), 1568 (s), 1487 (w), 1442 (s), 1401 (s), 1299 (s), 1281 (s), 1201 (s), 1116 (s), 1003 (w), 953 (w) 926 (m), 844 (s), 791 (s), 762 (m), 745 (s), 680 (s), 636 (m), 600 (w), 570 (w), 547 (m), 525 (w), 421 (s); ¹H-NMR (CDCl₃, 500 MHz): δ 4.06-4.10 (m, 3H, -CHF₂), 7.00 (s, 3H, Ar-H), 7.16-7.26 (d, 3H, Ar-H), 7.47-7.52 (d, 6H, Ar-H), 7.61-7.63 (d, 2H, Ar-H), 7.73-7.82 (d, 4H, Ar-H), 8.39-8.68 (d, 2H, Ar-H) ppm. Anal. Cal. for EuC₃₇H₂₃N₂O₉F₁₂: C, 43.59; H, 2.27; N, 2.75; Eu, 14.91; found: C, 43.58, H, 2.27; N, 2.75; Eu, 14.92.

2.4. Biological properties

(i) Evaluation of antimicrobial properties

The antibacterial action (in vitro) of L ligand and complexes were assessed towards the Gram-positive bacteria: *S. aureus* (Staphylococcus aureus), *B. subtilis* (Bacillus subtilis) and Gram-negative bacterium: *E. coli* (Escherichia coli) whereas antifungal activity was screened towards *C. albicans* (Candida albicans) and *A. niger* (Aspergillus niger) via tube dilution method.

The mediums of sabouraud dextrose I.P. (Indian Pharmacopoeia) and nutrient broth I.P. were utilized to prepare the dilutions of tested samples and reference drugs as used for antifungal screening (fluconazole) and antibacterial (ciprofloxacin), respectively in DMSO with 100 µg/mL concentration. The prepared dilutions of standard drugs and samples were left for incubation with different time durations and temperature such as 24 h (37 °C): bacterial strains, 48 h (37 °C): *C. albicans* and 7 days (25 °C): *A. niger*. The antimicrobial activity for ligand and complexes was determined by recording the minimum inhibitory concentration (MIC).

(ii) In vitro antioxidant activity

DPPH approach was applied to ascertain the antioxidant capacity of synthesized complexes and ligand L. DPPH (stable free radical) was reduced after accepting proton from the antioxidants resulting into violet color of DPPH changed to yellow color. The absorbance of resulting samples was monitored (at 517 nm) on ultraviolet-visible spectrophotometer. For antioxidant activity investigation, the solutions of tested complexes and standard (ascorbic acid) were prepared in ethanol with different concentrations (25, 50, 75 and 100) in µg/mL. The 1 mL ethanolic solution of DPPH (0.3 mM) was added to 1mL samples of various concentrations and then placed in dark (30 min) for incubation. The absorbance of samples with

different concentrations was documented with respect to blank solution and experiment was repeated in triplicate. The scavenging activity (% SCA) of free radical was reckoned by using following relation [11]:

$$\text{Scavenging activity (\%)} = [(Abs_{control} - Abs_{sample}) / Abs_{control}] \times 100 \quad (1)$$

In aforementioned relation, Abs_{sample} is noted absorbance for standard or samples+DPPH, $A_{control}$ denotes the absorbance of DPPH solution.

3. Results and discussion

3.1. Elemental investigation

The elemental analysis results clearly reveal the elemental (carbon, hydrogen, nitrogen) compositions of ligand and complexes (Table 1) while the presence of europium ion in complexes can be confirmed by performing special titration with ethylenediaminetetraacetic acid (EDTA).

Table 1. Compositions data of complexes of Eu^{3+} ion and ligand (L) in the form of weight %.

Complexes	C (%) found (cal.)	H (%) found (cal.)	N (%) found (cal.)	Eu (%) found (cal.)
L	45.38 (45.39)	2.52 (2.54)	-	-
C1	36.09 (36.06)	2.12 (2.13)	-	16.88 (16.90)
C2	51.22 (51.23)	2.63 (2.61)	2.35 (2.34)	12.72 (12.71)
C3	45.97 (45.95)	2.55 (2.54)	2.59 (2.61)	14.17 (14.18)
C4	44.89 (44.89)	2.21 (2.22)	2.69 (2.68)	14.56 (14.56)
C5	43.58 (43.59)	2.27 (2.27)	2.75 (2.75)	14.92 (14.91)

The EDAX spectrum (C5 complex) as illustrated in Fig. 1 determines the presence of elements (C, N, O, F and Eu) in this complex. It is suggested that the recorded data of elemental analysis and complexometric titration are concordant with theoretically calculated data and find close to the reported molecular formulae of ligand (L) and complexes (Scheme 1). The synthesized complexes are insoluble in water, diethyl ether and acetonitrile while completely soluble in DMSO.

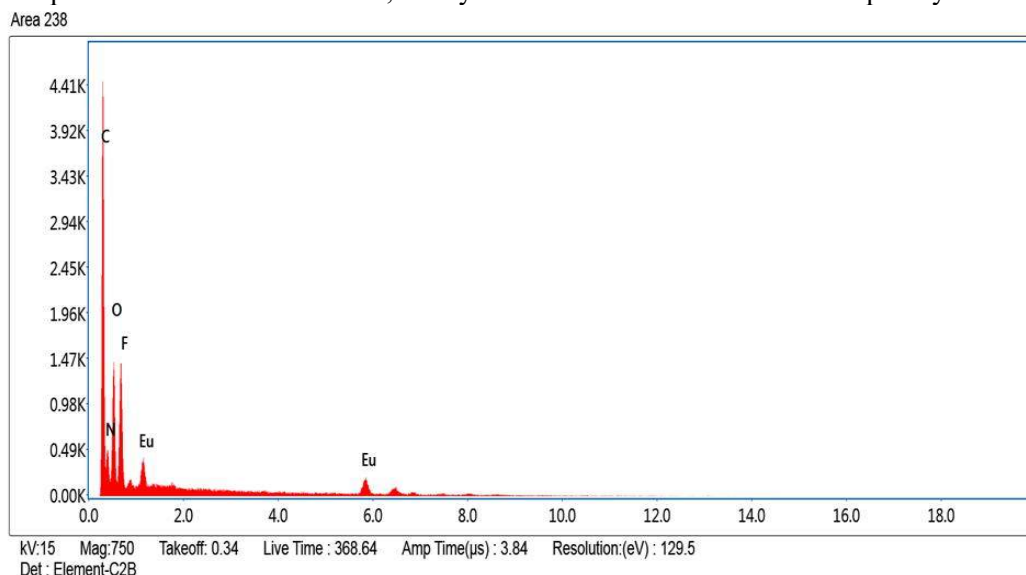


Fig. 1. EDAX spectrum of $[Eu(L)_3.bipy]$ i.e. C5 complex.

3.2. FT-IR and 1H -NMR spectral evaluation

The comparison of FT-IR spectral inspection for L ligand and its respective complexes corroborates the binding of L ligand to Eu^{3+} ion by displaying some noticeable changes. The important noted IR band frequencies are depicted in Table 2. FT-IR spectra of complexes have similar modes of binding of L ligand, hence, IR spectrum of C5 complex is observed the illustrative for all complexes.

Table 2. Major IR bands (cm^{-1}) for europium based complexes and uncoordinated L ligand.

Complexes	$\nu(\text{O-H})$	$\nu(\text{C=O})$	$\nu_{\text{asym}}(\text{OCO})$	$\nu_{\text{sym}}(\text{OCO})$	$\nu(\text{C=N})$	$\nu(\text{Eu-N})$	$\nu(\text{Eu-O})$
L	-	1705 (s)	-	-	-	-	-
C1	3426 (b)	-	1610 (s)	1443 (s)	-	-	425 (m)
C2	-	-	1633 (s)	1441 (s)	1566 (s)	571 (w)	420 (s)
C3	-	-	1635 (s)	1439 (s)	1544 (s)	573 (w)	423 (s)
C4	-	-	1634 (s)	1440 (s)	1545 (s)	573 (w)	423 (s)
C5	-	-	1633 (s)	1442 (s)	1568 (s)	570 (w)	421 (s)

b: broad, s: strong and w: weak

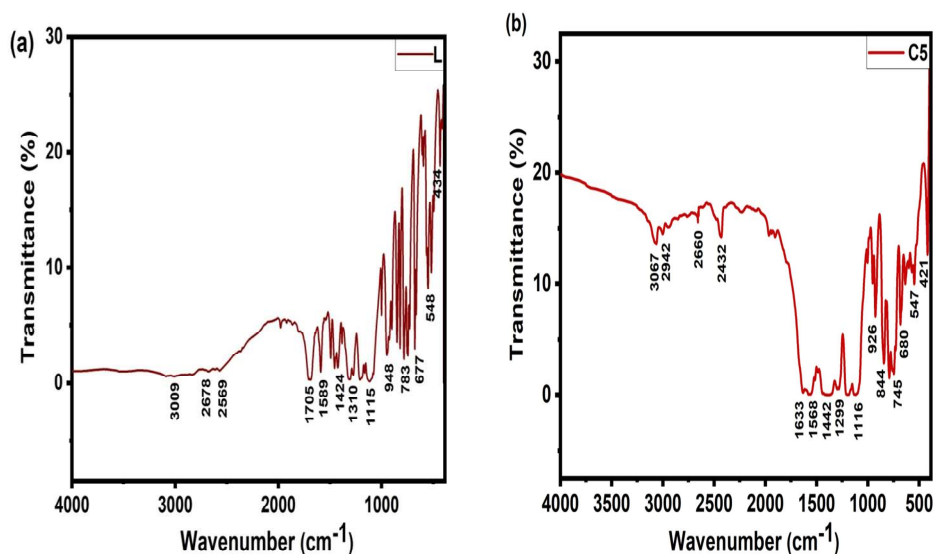


Fig. 2. (a) and (b) manifest the IR spectra of L ligand and C5 complex $[\text{Eu}(\text{L})_3\text{bipy}]$.

Fig. 2 portrays the IR spectra of L ligand (a) and illustrative complex (b). The stretching peaks centered at 1705 and 1274 cm^{-1} are imputed to carbonyl ($>\text{C=O}$) and C-F groups, respectively in free ligand L. On comparison with free ligand, IR spectra of complexes demonstrate the two new asymmetric (1610-1635 cm^{-1}) and symmetric (1439-1443 cm^{-1}) absorption bands for COO^- group irrespective of $>\text{C=O}$ band (at 1705 cm^{-1}) of carboxylic acid group in uncoordinated ligand (L), inferring the binding of ligand L to Eu^{3+} ion by COO^- ion. In addition, IR spectrum of binary complex reveals the visibility of a broad band at 3426 cm^{-1} on account of chelated water molecules accompanied by this complex. The difference of $\nu_{\text{asym, COO}^-}$ and $\nu_{\text{sym, COO}^-}$ stretching frequencies (167-196 cm^{-1}) favors the bidentate bonding mode of ligand to Eu^{3+} ion as defined by Deacon's rule [12]. The presence of a strong band due to Eu-O mode ranging from 420-425 cm^{-1} further affirms the involvement of ligand L in coordination reaction with europium(III) ion while the bands due to $>\text{C=N}$ group (1544-1568 cm^{-1}) and Eu-N (570-573 cm^{-1}) bond corroborate the binding of bidentate ancillary ligands with Eu^{3+} ion through nitrogen atoms in addition to L ligand.

$^1\text{H-NMR}$ spectral study further provides the detailed structural investigation of ligand L and complexes. The spectrum ($^1\text{H-NMR}$) for uncoordinated ligand L [**Fig. 3 (a)**] exhibits the peaks at δ 10.98, 8.04-8.06, 7.96, 5.80-6.08 ppm associated with the acidic proton, aromatic proton nearer to OCF_2CHF_2 group, aromatic protons and CHF_2 proton, respectively. Another

singlet resonance peak is also visible at δ 7.26 ppm due to CDCl_3 solvent. On complexation, the vanishing of resonance peak of acidic proton (δ 10.98 ppm) is consistent with the chelation of ligand L (through deprotonated acidic group) to $\text{Eu}(\text{III})$ ion. On the other hand, the resonance peaks corresponding to $-\text{CHF}_2$ and aromatic protons are slightly shifted to upfield of δ 2.18-4.10 and 7.32-7.35 ppm, respectively, which indicates the involvement of acidic group in coordination with Eu^{3+} ion. The chelation of ancillary ligands to trivalent europium ion can be substantiated with the visibility of some new peaks of aromatic protons ranging from δ 8.09-8.18 and 8.39-9.03 ppm in spectra of ternary complexes. The alignment of resonance peaks in ^1H -NMR spectra of all complexes are of same manner, henceforth, the spectral study is defined by complex C4 spectrum manifested in **Fig. 3 (b)**.

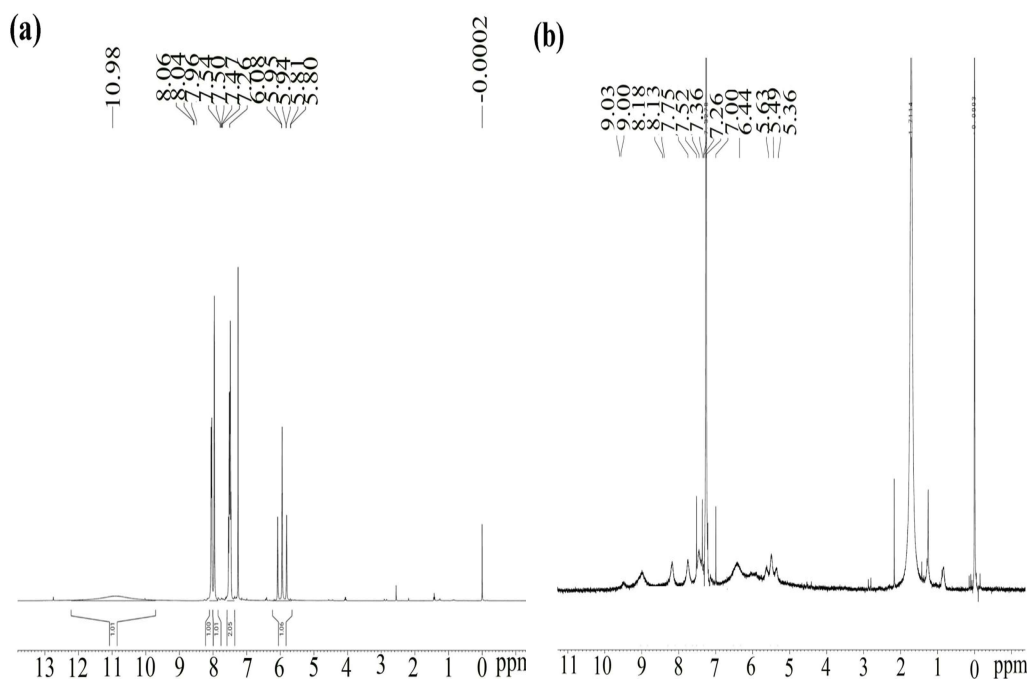


Fig. 3. Demonstration of proton NMR spectra of ligand L (a) and C4 complex (b) $[\text{Eu}(\text{L})_3.\text{phen}]$.

3.3 Thermal stability determination

Thermal (TG/DTG) curves determine the thermal behavior of complexes. Thermal stability curve of C5 complex (**Fig. 4**) is taken as explanatory of all synthesized complexes because all complexes are decomposed in same order. The thermographs (TG and DTG) of C5 complex indicate that the complex is decomposed in two stages. The initial stage of decomposition is specified by evaporation of moisture with 3.71 % weight loss up to 306 $^{\circ}\text{C}$. After evaporation of moisture, thermal stability curves mention the elimination of one molecule of bipy ancillary ligand and three molecules of L ligand (coordinated to Eu^{3+} ion in chelated scaffold) up to 520 $^{\circ}\text{C}$ with loss of weight 84.14 %. The europium oxide remains as last product. The thermal study proclaims the thermal stability (around 306 $^{\circ}\text{C}$) for complexes, thus it substantiates the successful implementation of these complexes in fabrication of photonic devices.

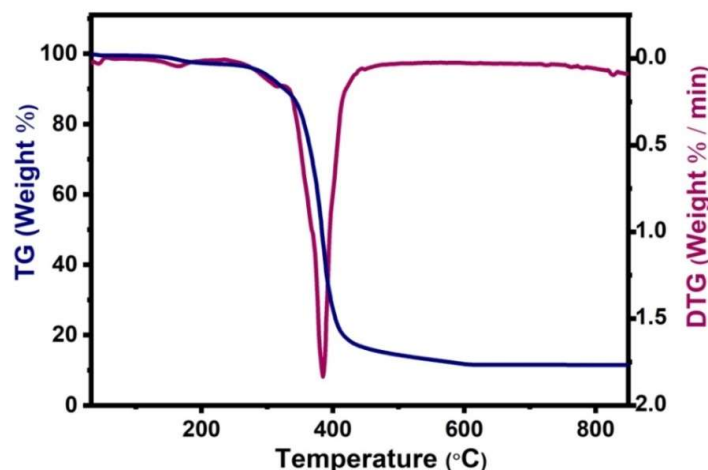


Fig. 4. Manifestation of DTG and TG analysis for europium based C5 complex.

3.4 Optoelectronic features

Electronic absorption spectra of L and its corresponding complexes of trivalent europium ion are scanned in 200-800 nm range evinced in **Fig. 5**. The spectral record of ligand (L) and complexes demonstrate similar spectral profile but complexes display small extent of perturbation as compared to ligand. The absorption bands of ligand ranging from 245-259 nm and 259-300 nm with maxima of 251 nm and 272 nm are ascribed to ligand centered transitions. The absorption bands of complexes show the red shift (20-43 nm and 14-36 nm) in wavelength than that of ligand due to formation of enlarged conjugated structure in the complexes. This red shift in complexes supports the migration of energy from ligand to Eu^{3+} ion [13].

The solid excitation spectra of complexes are recorded in wavelength span of 200-500 nm at room temperature under slit width of 2.5 nm (voltage of 400 PMT) at emission wavelength of 613 nm or 614 nm corresponding to most intense transition $^5\text{D}_0 \rightarrow ^7\text{F}_2$. The excitation spectra of the complexes (**Fig. 6**) mainly comprise a broad band positioned with spanning of 250-386 nm having maxima of 357 nm (C1), 362 nm (C2-C4) and 340 nm (C5). The broad band is possibly allocated to ligand oriented transition ($\pi \rightarrow \pi^*$) and two weak bands peaking at 395 nm ($^7\text{F}_0 \rightarrow ^5\text{L}_6$) and 469 nm ($^7\text{F}_0 \rightarrow ^5\text{D}_2$) are imputed to electronic transitions of trivalent europium ion, respectively [14].

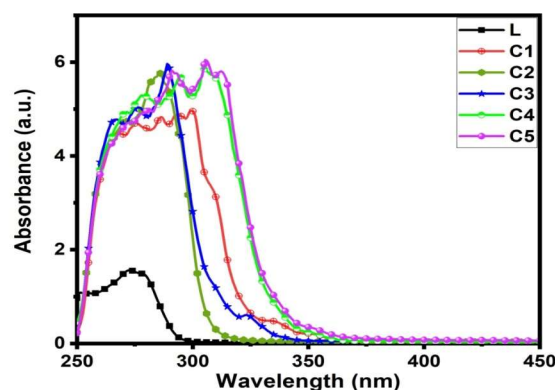


Fig. 5. Electronic absorption spectral profile for L (ligand) and its corresponding complexes of Eu^{3+} ion.

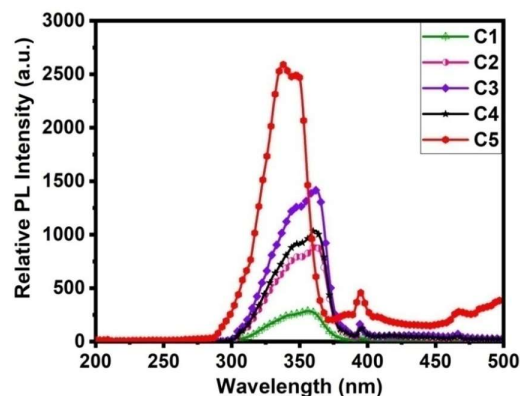


Fig. 6. Excitation spectra of europium complexes under 613 or 614 nm emission wavelength.

The emission spectra of complexes are documented at corresponding excitation wavelength. The characteristic emission peaks corresponding to transitions from 5D_0 (ground) level to $^7F_{0,1,2,3,4}$ (excited levels of Eu^{3+} ion) are centered at 580 nm, 591 nm (C1-C4 and 592 nm for C5), 613 nm (C4-C5 or 614 nm for C1-C3), 651 nm (C1, C3-C5 and 657 nm for C2) and 687 nm (C1-C3, 688 for C5 and 694 nm for C4), respectively as demonstrated in emission spectra of complexes (Fig. 7). The transition related to most intense peak (613 or 614 nm) is characterized as forced ED (electric dipole) transition which is more susceptible to surrounding environment and responsible for highly red color purity of Eu^{3+} ion [15]. The second intense peak at 591 or 592 nm imputed to MD (magnetic dipole) transition is insusceptible to chemical environment surrounding the Eu^{3+} ion and consequently it can be utilized as an internal standard calibration for other emission peaks. Notably, the emission intensity of ED transition is relatively higher irrespective of MD transition, it corroborates that the central europium lacks of inversion center in surrounding coordination environment. Besides, the less intense peaks at 469, 536 (C4, 537 nm: C1-C3, C5) and 555 nm (C1-C3, C5, 557 nm: C4) are accountable for $^5D_2 \rightarrow ^7F_0$, $^5D_1 \rightarrow ^7F_0$, $^5D_1 \rightarrow ^7F_2$ transitions, respectively. The transition of $^5D_0 \rightarrow ^7F_0$ is referred to as symmetric forbidden transition because this is not allowed by ED as well as MD mechanism. The luminosity of ternary complexes is significantly boosted by saturation of coordination scaffold of C2-C5 complexes through embedding the ancillary ligands by replacing solvent (water) molecules present in binary complex. It is worthwhile to note that the ancillary ligands occupied by ternary complexes restrict the energy dissipation produced by lattice vibration of water molecules (through O-H oscillators) situated in the close vicinity of Eu^{3+} ion, which leads to reinforce luminosity of ternary complexes. Henceforth, these complexes are utilized as efficient luminous materials in lighting devices.

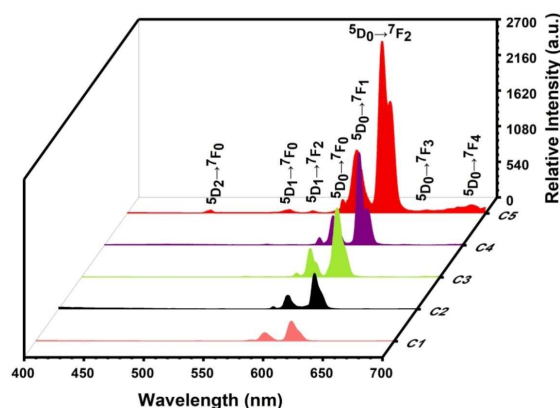


Fig. 7. Emission spectra of complexes of trivalent europium ion at corresponding excitation wavelength.

Further, branching ratio confirm the photoluminescence efficiency of complexes, it is evaluated on dividing the integral intensity of individual peak to the sum of integral intensity of all emission peaks (emanating from europium centered 5D_0 level). The branching ratios of complexes are spanning between 69.80-73.17 % (Table 3) with respect to most intensive transition $^5D_0 \rightarrow ^7F_2$ (electric dipole transition), which are found to be greater than 60 %, indicates that the complexes play a significant role in laser technology [16].

Table 3. Branching ratio of europium complexes corresponding to different types of electronic transitions.

Complexes	$^5D_0 \rightarrow ^7F_0$	$^5D_0 \rightarrow ^7F_1$	$^5D_0 \rightarrow ^7F_2$	$^5D_0 \rightarrow ^7F_3$	$^5D_0 \rightarrow ^7F_4$	I_{614}/I_{591}
C1	1.95	27.29	69.80	0.19	0.74	2.56
C2	2.22	26.58	70.00	0.42	0.78	2.63
C3	1.80	24.14	73.17	0.37	0.53	3.03
C4	2.99	23.24	72.06	0.77	0.94	3.10
C5	23.82	22.22	71.63	0.91	2.86	3.22

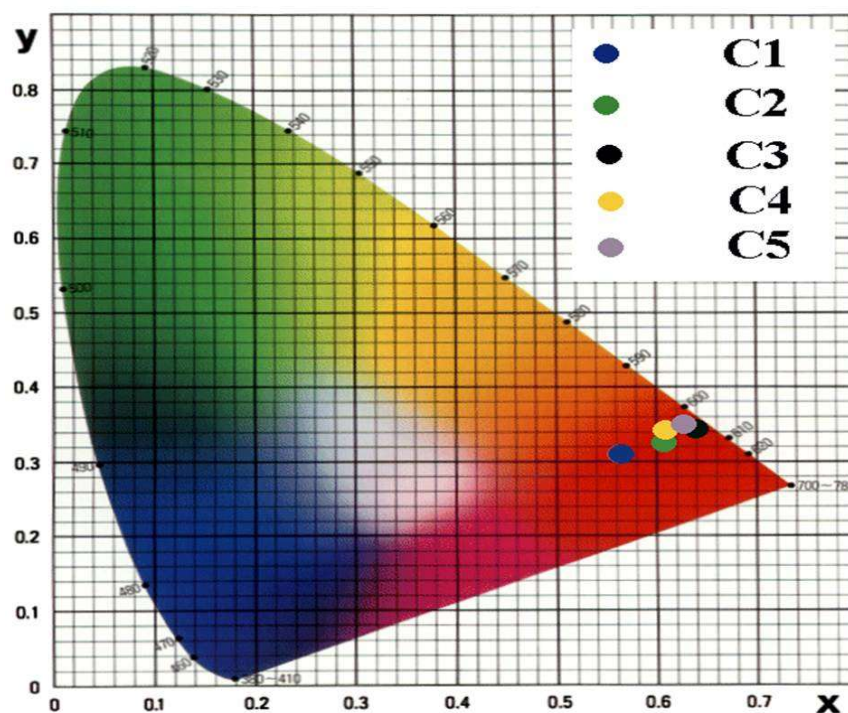


Fig. 8. Representation of chromaticity coordinates of europium complexes located in red region.

The chromaticity coordinates certify the emitted color of Eu(III) complexes which are reckoned via MATLAB software upon feeding the emission data and observed coordinates are tabularized in Table 4. Fig. 8 clearly reflecting the existence of color coordinates in red zone for complexes and in close approximation (C3 and C5 complexes) with National Television System Committee (NTSC) coordinates (0.64, 0.34).

Table 4. Color purity (p_c) and CIE coordinates of europium(III) complexes.

Complexes	C1	C2	C3	C4	C5
CIE coordinates	x = 0.569	x = 0.612	x = 0.643	x = 0.612	x = 0.632
(x, y)	y = 0.311	y = 0.334	y = 0.351	y = 0.342	y = 0.354
p_c (%)	67.64	80.58	94.94	86.13	93.04

Table 5. Decay time (τ), refractive index (n), optical band-gap (E_g) and photoluminescent data of complexes.

Complexes	τ (ms)	A_{rad} (s^{-1})	A_{nrad} (s^{-1})	$\Omega_{2,4}$ ($10^{-20}cm^2$)	η (%)	E_g (eV)	n
C1	0.6741	188.37	1295.09	2.94, 0.04	12.70	3.91	1.88
C2	0.8937	193.51	925.43	3.03, 0.04	17.29	3.88	1.88
C3	1.1256	212.99	675.42	3.48, 0.03	23.97	3.76	1.90
C4	1.1386	221.29	656.98	3.56, 0.05	25.20	3.50	1.94
C5	1.6523	231.88	373.34	3.69, 0.17	38.31	3.37	1.97

The luminance property is also confirmed by determination of color purity (p_c) of that particular emission color, which is systematically calculated by extending a line through the midpoint of respective complex coordinates (x_s, y_s) and white color coordinates ($x_i = 0.333, y_i = 0.333$) and the point at which line crosses the chromaticity diagram produces x_d, y_d (dominant coordinates). The color purity (p_c) can be enumerated by using following relation [17]:

$$Color\ purity = \frac{\sqrt{(x_s - x_i)^2 + (y_s - y_i)^2}}{\sqrt{(x_d - x_i)^2 + (y_d - y_i)^2}} \times 100\% \quad (2)$$

The calculated data of p_c (67.64-94.94 %) for the complexes are depicted in **Table 4**, which proposes the comparatively smaller value of p_c of binary complex in comparison to ternary complexes. This is due to intensification of luminescence through extending conjugation by using ancillary ligands in ternary complexes. Thus, it remarks the role of complexes as efficient red color emitter in preparation of white light emitting diodes.

The decay curves further affirms the optical properties of complexes, which can be recorded by monitoring the emission wavelength (613 nm or 614 nm) and respective excitation wavelength. The decay curves essentially follow the mono-exponential model as illustrated by the following expression [18]:

$$I(t) = I_0 + A_1 \exp(-t / \tau) \quad (3)$$

In aforementioned expression, A_1 denotes a scalar quantity, $I(t)$ epitomizes the integrated area at t time, I_0 signifies the offset value and τ depicts the emissive lifetime. The emissive lifetime (τ) for excited level 5D_0 of europium(III) ion are calculated from the mono-exponential function and found to be 0.6741-1.6523 ms compiled in **Table 5**. The mono-exponential nature of decay curves as embodied in **Fig. 9** suggests the presence of single dominant europium ion in complexes. The enhancement of emissive lifetime from binary to ternary complexes further underscores the luminescence performance of these complexes. This increased lifetime of ternary complexes is supported by saturation of coordination scaffolds of ternary complexes by ancillary ligands by exchanging coordinated water molecules in binary complex, which avoids the non-radiatively deactivation of excited states and enhance the lifetime of ternary complexes.

The radiative transition rate (A_{0j}) of emission peaks ascribed to $^5D_0 \rightarrow ^7F_{J=0,1,2,3,4}$ transitions is reckoned in accordance with the following relation [19]:

$$A_{0j} = A_{01} \left(\frac{I_{0j}}{I_{01}} \right) \left(\frac{\nu_{01}}{\nu_{0j}} \right) \quad (4) \quad \text{Where}$$

I_{0j} denotes the integrated intensity, ν_{0j} is the maxima of emission peaks (cm^{-1}) whereas A_{01} typifies the coefficient for spontaneous emission with respect to $^5D_0 \rightarrow ^7F_1$ transition ($A_{01} \sim 50s^{-1}$) and it is implemented as internal reference for determination of radiative transition rate (A_{0j}) for all transitions. Total radiative transition rate (A_{rad}) defines the summation of individual transition rate (A_{0j}) as given below [20]:

$$A_{rad} = \sum_{j=0,1,2,3,4} A_{0j} = A_{00} + A_{01} + A_{02} + A_{03} + A_{04} \quad (5)$$

Total transition rate (A_t) belongs to the addition of A_{nrad} (non-radiative transition rate) and A_{rad} as according to given relation and its value also represented by reciprocal of emissive lifetime (τ).

$$A_t = 1/\tau = A_{rad} + A_{nrad} \quad (6)$$

The internal quantum efficiency (η) substantiates the luminescence performance of europium complexes, which is estimated by utilizing the given expression:

$$\eta = \frac{A_{rad}}{A_{rad} + A_{nrad}} = \frac{A_{rad}}{A_{total}} \quad (7)$$

The calculation regarding evaluation of internal quantum efficacy (η) is made successfully and calculated values are compiled in **Table 5**. The internal quantum efficacy of ternary complexes (17.29-38.31 %) can be improved by the inserting ancillary ligands in chelated scaffold of these complexes, which subdues the energy transfer non-radiatively process. The better luminance efficacy of these complexes extends their practical applications in display devices as well as in optoelectronic devices.

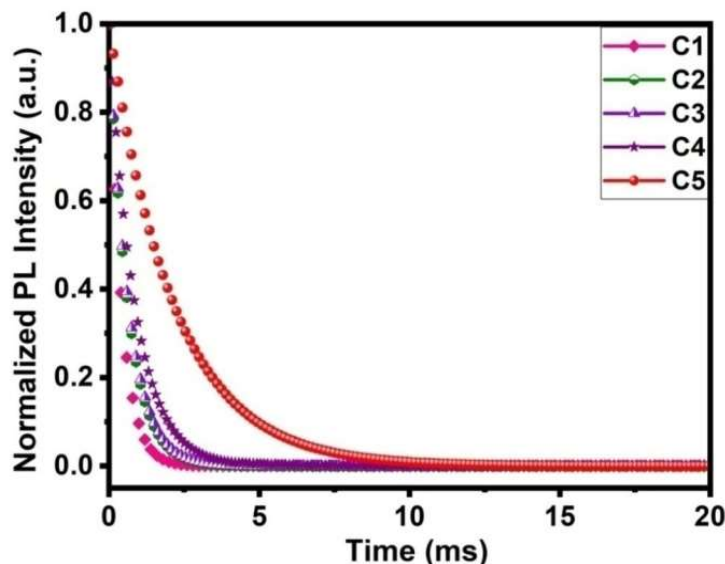


Fig. 9. demonstrates the decay curves of europium complexes at room temperature.

In order to get further information regarding the chemical environment around central trivalent europium ion, Judd-Ofelt intensity parameters (J-O) of the complexes are evaluated for electric dipole transitions $^5D_0 \rightarrow ^7F_J$ ($J = 2, 4, 6$) obtained in emission spectra of complexes. J-O parameters are enumerated according to given expression by putting the value of $\langle ^5D_0 | U^\lambda | ^7F \rangle^2$ (square reduced matrix element) for different transitions [$\langle ^5D_0 | U^\lambda | ^7F \rangle^2 = 0.0034$ and $\langle ^5D_0 | U^\lambda | ^7F \rangle^2 = 0.0023$] [21].

$$\Omega_\lambda = \frac{3.h.(2J+1).A_{0J}}{64.\pi^4.e^2.\bar{\nu}^3.\chi.\langle ^5D_0 | U^\lambda | ^7F \rangle^2} \quad (8)$$

In above mentioned expression, e denotes the electronic charge (4.80×10^{-10} esu), χ demarcates Lorentz field correction term which is illustrated by $n(n^2 + 2)^2/9$, $\bar{\nu}$ is the average wavenumber of the transitions and h represents Planck's constant. The value of n (refractive index) for europium complexes is used as ~ 1.5 . Eventually, the estimation of J-O parameters is made successfully while the reliable determination of Ω_6 is not possible as $^5D_0 \rightarrow ^7F_6$ transition is not detected in emission spectra. The resulting values of Ω_2 and Ω_4 are enlisted in **Table 5**, which clearly demonstrates the comparatively higher value of Ω_2 for ternary complexes (3.03 - $3.69 \times 10^{-20} \text{ cm}^2$) as compared to binary complex ($2.94 \times 10^{-20} \text{ cm}^2$) owing to the rigid framework provided by ancillary ligands in ternary complexes. The value of Ω_2 is more sensitive to small angular changes local environment around the central Eu^{3+} ion while Ω_4 is more sensitive to coordinated ligand and central europium(III) ion distance.

3.5. Morphological features

The surface topography of particles exhibited by the complexes is visualized by SEM image. The SEM image of C5 complex (**Fig. 10**) clearly shows that the fluffy mass of particles is present in agglomeric stage and particles are arranged in high packing density which decreases the chances of scattering of light and enhances the luminescence performance of synthesized complexes.

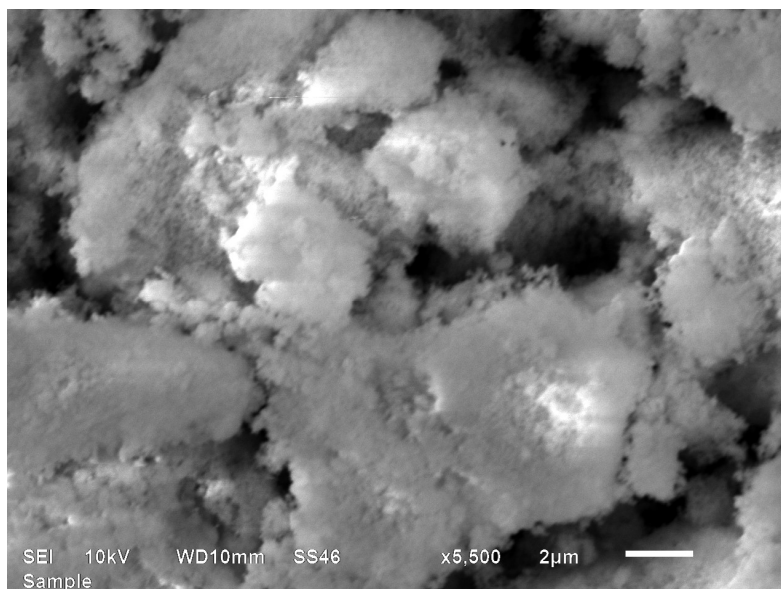


Fig. 10. SEM image of complex C5, Eu(L)₃.bipy.

3.6. Band-gap and refractive index scrutiny

Diffuse reflectance spectra of L ligand and its respective complexes are recorded at room temperature, which are putting into Kubelka-Munk function to enumerate the band-gap energy of complexes and ligand. The band-gap (E_g) confirms the semiconductor property of the complexes and it is estimated by using following expression [22]:

$$[\alpha h\nu]^n = C(h\nu - E_g) \quad (9) \text{ In aforementioned equation,}$$

C is the constant of proportionality, $h\nu$ denotes the energy of photons, $n = 2$ for direct allowed transition and α represents Kubelka-Munk function which is shown by the given relation:

$$\alpha = \frac{(1 - R_\infty)^2}{2R_\infty} = K/S \quad (10)$$

Where R_∞ demonstrates the observed reflectance and K/S denotes the ratio of absorption coefficient (K) and scattering coefficient (S). The tangential extrapolation of $(\alpha h\nu)^2 = 0$ against photon energy ($h\nu$) estimates the optical band-gap (**Table 5**) of complexes (3.91-3.37 eV) and ligand (4.11 eV). The E_g values of complexes are comparable to that of wide band-gap semiconductors i.e. 2-4 eV, which makes them unique candidate for the applications in energy converting systems and military radar. **Fig. 11** depicts Tauc plots for L (**a**) and C5 complex (**b**) whereas insets present their respective diffuse reflectance spectra.

In addition, the complexes are characterized by the determination of refractive index (n) with utilization of E_g as exemplified by given equation [23]:

$$n^2 - 1/n^2 + 1 = 1 - \sqrt{E_g/20} \quad (11)$$

The range of refractive index for complexes is found to be 1.88-1.97 (**Table 5**) which is in approximation to that of other luminescent materials [$n = 2.03$: Tb(HEAP)₃.2H₂O, $n = 1.5256$: Eu(BA)(TTA)₂.phen] and the resulting n values of complexes proves the suitability of these complexes in fabrication of optic fibers as well as optoelectronic devices.

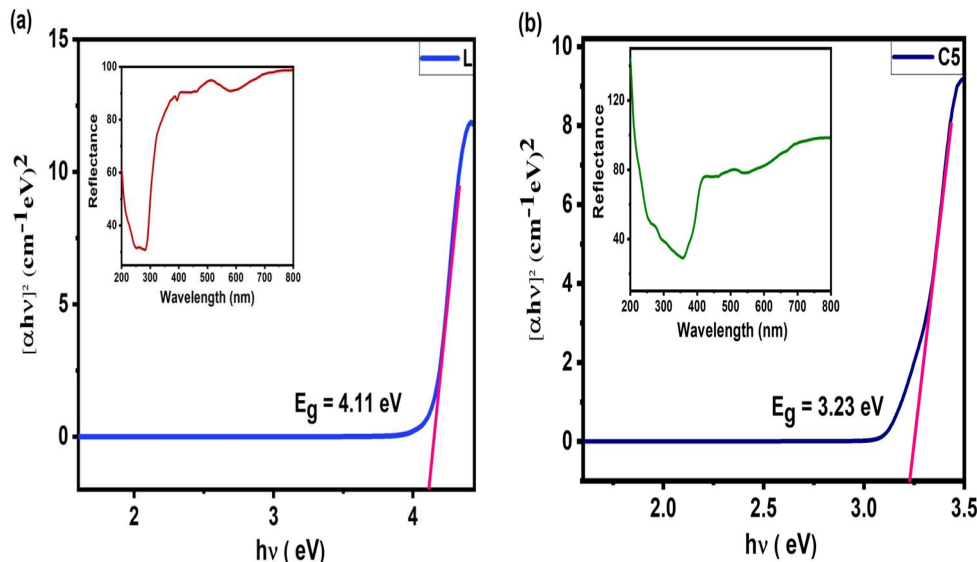


Fig. 11. Tauc plots of L ligand (a) and complex C5 (b) and their diffuse reflectance spectra represent in insets of these figures.

3.7. Investigation of biological features

(i) Antimicrobial features

The antimicrobial (antibacterial and antifungal) activity of ligand and complexes are assessed in terms of MIC values (**Table 6**). **Table 6** clearly exposes that the complexes demonstrate the excellent bactericidal and fungicidal activity irrespective of ligand and standard drugs. The antimicrobial potential is illustrated in **Fig. 12** (C5 complex). Against *S. aureus*, C2 complex (MIC = 6.23 µg/mL) is emerged as a more potent agent, complexes C3-C5 demonstrate moderate antibacterial potential with MIC value of 12.5 µg/mL and least reactivity is shown by C1 complex (MIC = 25.0 µg/mL). The excellent potential of complex C4 (MIC = 6.25 µg/mL) helps to retard the growth of *B. subtilis* to a greater extent whilst C2-C3 complexes (MIC = 10.7 µg/mL) disclose the moderate action towards this bacterial pathogen and antibacterial action of C1 and C5 complexes (MIC = 25.0 µg/mL) are turned out to be poor and comparable to ciprofloxacin (standard drug). The antibacterial potential of C3 complex (MIC = 6.25 µg/mL) is found to be effective against *E. coli*, C4 complex (MIC = 10.7 µg/mL) exhibits moderate bactericidal activity and the complexes C2 and C5 (MIC = 12.5 µg/mL) are least active to suppress the growth of this pathogen but more active than C1 complex (25.0 µg/mL). The complexes C2 and C4 act as excellent fungicides against *C. albicans* with value of 6.23 µg/mL (MIC) whereas the moderate antifungal action is shown by C5 complex (MIC = 6.25 µg/mL) and complexes C1 (10.7 µg/mL) and C3 (12.5 µg/mL) are least capable to inhibit the action of this fungal pathogen. The better antifungal activity is shown by C2 complex (MIC = 6.25 µg/mL) for *A. niger* fungal strain as compared to other complexes. The recorded results clearly indicate the higher antimicrobial potential of complexes as compared to free ligand L. It is noted that the ligand is shared its own electron density with central Eu^{3+} ion after undergoing complexation with Eu^{3+} ion, which results into damaging the permeability and integrity of microorganisms membrane and inhibit the growth of microorganism. This enhanced antimicrobial efficacy of complexes proves their appropriateness in application of bioimaging.

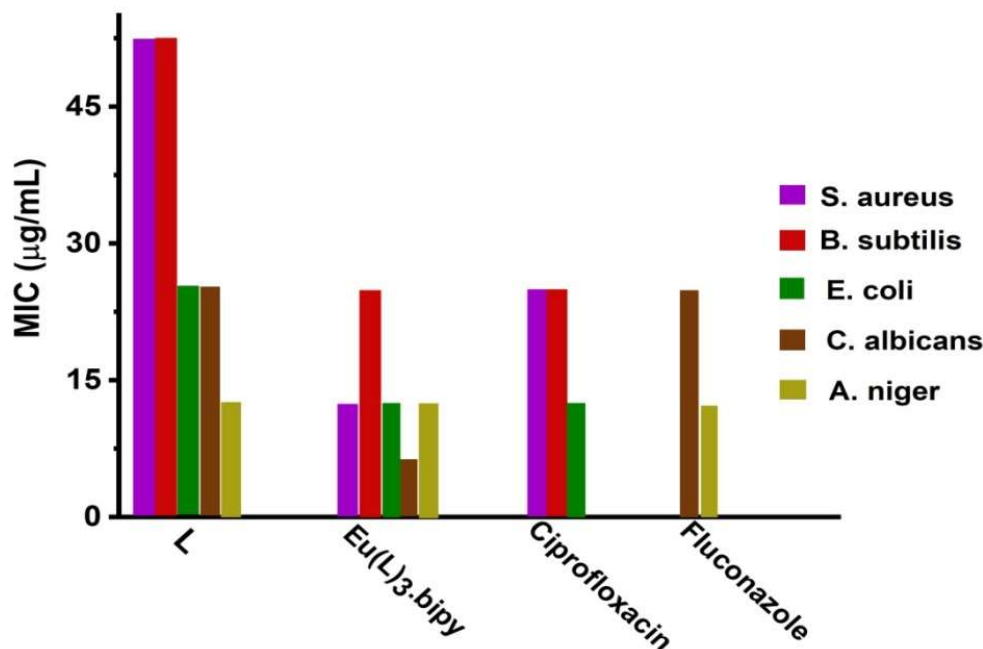


Fig. 12. Representation of antimicrobial activity of ligand (L) and C5 complex against standard drugs (ciprofloxacin and fluconazole).

(ii) Antioxidant features

The antioxidant activity of ligand and complexes is scrutinized in the form of IC_{50} (half maximal inhibitory concentration) values which are determined from the graph plotted between concentration and percentage scavenging activity. IC_{50} values of ligand L, complexes and standard (ascorbic acid) are recorded in Table 7. The plot of radical scavenging activity (% SCA) against different concentrations is portrayed in Fig. 13. The compiled data of Table 7 corroborates that the IC_{50} values of complexes (48.75-61.53 $\mu\text{g/mL}$) are comparatively lower than ligand (67.59 $\mu\text{g/mL}$) and lower IC_{50} values signify the greater antioxidant potential of the complexes. The ternary complexes ($IC_{50} = 48.75\text{-}57.78 \mu\text{g/mL}$) demonstrate the good radical scavenging activity as compared to binary complex ($IC_{50} = 61.53 \mu\text{g/mL}$). This is due to the presence of highly conjugated system in ternary complexes (on account of ancillary ligands), which increases the delocalization of π -electron cloud over the complete chelated ligand and improves the antioxidant potential of ternary complexes.

Table 6. Minimum inhibitory concentration (MIC) values for L ligand and europium complexes. Highest antimicrobial activity is shown by bold values.

Complexes	Minimum inhibitory concentration ($\mu\text{g/mL}$)				
	MIC _{sa}	MIC _{bs}	MIC _{ec}	MIC _{ca}	MIC _{an}
L	50.0	50.0	25.0	25.0	12.5
C1	25.0	25.0	25.0	10.7	12.5
C2	6.23	10.7	12.5	6.23	6.25
C3	12.5	10.7	6.25	12.5	10.7
C4	12.5	6.25	10.7	6.23	10.7
C5	12.5	25.0	12.5	6.25	12.5
SD	25.0 ^a	25.0 ^a	12.5 ^a	25.0 ^b	12.5 ^b

a: ciprofloxacin, b: fluconazole, ca: Candida albicans, an: Aspergillus niger, ec: Escherichia coli, bs: Bacillus subtilis and sa: Staphylococcus aureus

Table 7. depicting the percentage scavenging activity (%) and IC₅₀ values of L ligand and complexes.

Complexes	Concentration (µg/mL)					IC ₅₀
	25	50	75	100		
L	24.16	39.96	53.58	70.06		67.59
C1	28.38	42.90	58.25	72.77		61.53
C2	34.47	50.79	67.19	83.69		48.75
C3	31.06	46.36	62.69	77.78		55.46
C4	33.62	49.55	64.74	80.07		51.20
C5	30.98	45.63	59.80	74.83		57.78
Ascorbic acid	35.87	52.16	68.35	85.27	46.71	

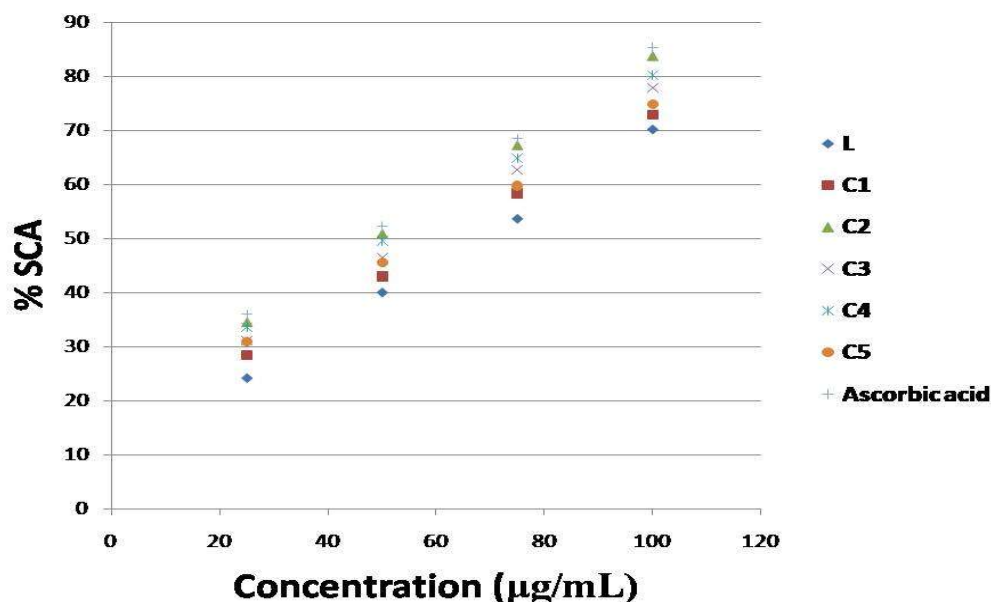


Fig. 13. Variation of percentage scavenging activity (% SCA) with concentration (µg/mL) for standard ascorbic acid, L ligand and complexes.

3.8. Photosensitized energy transfer mechanism

The most probable mechanism of energy transfer determines the photoluminescence efficiency of complexes, which firstly involves the absorption of photons by ligand in its ground singlet state (S_0) and then excites to excited singlet state (S_1). The S_1 state migrates optimal energy to its respective lowest excited triplet state (T_1) through intersystem crossing (ISC) pathway after that ligand's T_1 state feeds the excited electronic levels (resonating levels) of europium(III) ion. The resonating levels undergo relaxation via non-radiative decay process and produce luminescence in the visible region. The complete energy transfer pathway follows some phenomenological rules. In first rule, the appropriate energy difference between S_1 and T_1 states should be observed around 5000 cm^{-1} (0.62 eV) [24]. In second rule, energy transfer rate solely relies upon the position of ligand centered T_1 state which should lie above the position of resonating levels of metal ion. In this regard, a safe energy difference between excited resonating level of metal ion and nearby T_1 state should be accepted within the range of $2000\text{--}5000\text{ cm}^{-1}$ ($0.25\text{--}0.62\text{ eV}$) as per Latva rule [25]. Therefore, to elucidate the energy transfer mechanism, position of S_1 and T_1 states of L ligand can be systematically evaluated by considering the absorption spectrum (**Fig. 5**) of ligand and phosphorescence spectrum (**Fig. 14**) of gadolinium complex of L ligand [G_1 : $Gd(L)_3 \cdot H_2O$] as references, respectively, which are computed as 32258 cm^{-1} (4.00 eV) and 24272 cm^{-1} (3.01 eV) and epitomized in **Table 8**.

Table 8. Energy states of ligands and energy difference between these states of ligands and resonating levels of Eu^{3+} ion (cm^{-1}).

Ligands	(S_1)	(T_1)	$\Delta E_0(S_1-T_1)$	$\Delta E_1(T_1-^5D_0)$	$\Delta E_2(T_1-^5D_1)$
L	32258	24272	7986	7031	5650
Bipy	29900	22900	7000	5659	4278
Phen	31000	22100	8900	4859	3478
Batho	29000	21000	8000	3759	2378

5D_0 and 5D_1 : resonating levels of Eu^{3+} ion, S_1 and T_1 : lowest excited singlet and triplet states of ligands

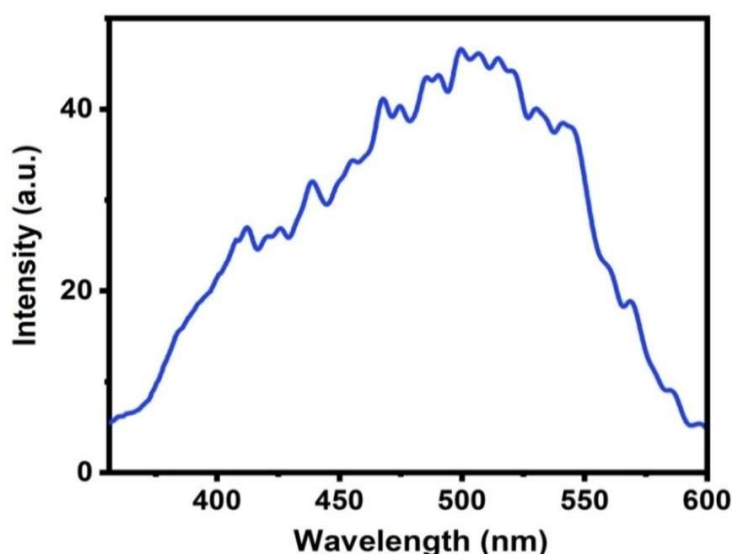


Fig. 14. Phosphorescence emission spectrum of gadolinium complex of L ligand.

The values of S_1 and T_1 states for ancillary ligands batho, phen and bipy are estimated by using same procedure as used for ligand L and enlisted in **Table 8**, which are finely matched with the already reported in literature [20]. On the basis of above discussed rules, a schematic energy transfer pathway is constructed and displayed in **Fig. 15** (for C5 complex). Taking into account the first empirical rule, the energetic difference (ΔE_0) between S_1 and T_1 states of L ligand is 7986 cm^{-1} (0.99 eV) which indicates a concern for effective ISC. Meanwhile, the difference of energy for T_1 state of feeding ligand L and resonating levels 5D_0 (17241 cm^{-1} : 2.14 eV), 5D_1 (18622 cm^{-1} : 2.31 eV) and 5D_2 (21322 cm^{-1} : 2.64 eV) of trivalent europium ion is considered to be 7031 (0.87 eV), 5650 (0.70 eV) and 2950 cm^{-1} (0.36 eV), respectively. This difference of energy is acceptable for 5D_2 resonating level (according to Latva rule), whereby the ligand L sensitizes the Eu^{3+} ion and reinforces the luminescence efficacy of the complexes. The 5D_0 resonating level is populated by 5D_2 level via non-radiative decay aisle and subsequently it gets relax to 7F_1 ground levels of Eu^{3+} ion by producing luminescence in visible region through radiative decay process. The ΔE_2 values for different ancillary ligands are estimated to be 4278 cm^{-1} (0.53 eV: bipy), 3478 cm^{-1} (0.43 eV: phen) and 2378 cm^{-1} (0.29 eV: batho), which promises the efficient rate of energy transfer in case of C5 complex with bipy ancillary ligand, leading to strengthening the luminescence performance of that complex. While the lowest ΔE_2 value for batho ancillary ligand is responsible for back transfer of energy from resonating level of Eu(III) ion to T_1 state of batho ancillary ligand, which accounts for least luminosity of C2 complex among all ternary complexes. Although dmph and phen ancillary ligands possess same structural framework, the dmph ancillary ligand is enriched by two additional methyl groups as compared to phen ancillary ligand, which increase the non-radiatively energy loss (via vibronic quenching of C-H bond) and act as quencher of luminosity for C3 complex, thus the luminescence efficacy of C3 complex is declined in comparison to C4 complex [47].

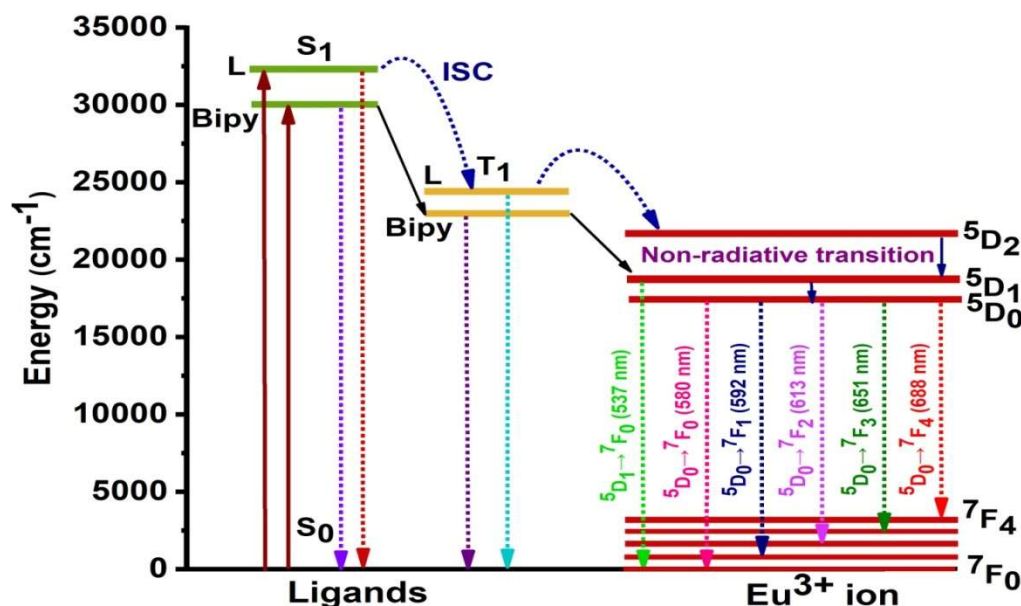


Fig. 15. Energy diagram showing the excited states of ligand and resonating levels of Eu^{3+} ion and sensitization of europium ion by ligands.

Conclusion

This research work reflects the synthesis of new family of europium based complexes with inculcation of fluorinated aromatic acid (L) and different types of ancillary ligands in coordination sphere. The coordination of ligand is substantiated by using different spectral techniques of EDAX and elemental analysis, FT-IR and $^1\text{H-NMR}$. Thermal analysis unveils the higher thermal stability (306°C) of these synthesized complexes, which confirms the utility of complexes in photonic devices. The intense red emission is shown by the electronic transition of $^5\text{D}_0 \rightarrow ^7\text{F}_2$ (613 or 614 nm) of $\text{Eu}(\text{III})$ ion. The quantum efficiency and emission intensity of ternary complexes can be reinforced by using ancillary ligands in addition of main ligand L because ancillary ligands saturate the coordination sphere by replacing solvent molecules present in coordination sphere of binary complex. Thus these complexes are successfully implemented in preparation of new generation lighting devices and LSCs. Judd-Ofelt parameter (Ω_2) for europium complexes are calculated as $2.94\text{--}3.69 \times 10^{-20} \text{ cm}^2$. The uniform packing of particles in complexes is validated by SEM analysis. The band-gap determination for complexes (3.91–3.37 eV) reveals the semiconducting properties of synthesized complexes. The significant sensitization of central europium ion by ligand L is proved by interpretation of energy transfer mechanism. In last, the complexes are acting as potent antimicrobes and antioxidant agents.

Acknowledgement

There is no funding source from any agencies for this research work.

References

- [1] Hasegawa, Y. (2014). Photofunctional lanthanoid complexes, coordination polymers, and nanocrystals for future photonic applications. *Bulletin of the Chemical society of Japan* 87, 1029–1057.
- [2] Bunzli, J.C.G. & Piguet, C. (2005). Taking advantage of luminescent lanthanide ions. *Chemical Society Reviews* 34, 1048–1077.
- [3] Hewitta, S.H. & Butler, S.J. (2018). Application of lanthanide luminescence in probing enzyme activity. *Chemical Communications* 54, 6635–6647.
- [4] Assadi, M.K., Hanaei, H., Mohamed, N.M., Saidur, R., Bakhoda, S., Bashiri, R. & Moayedfar, M. (2016). Enhancing the efficiency of luminescent solar concentrators (LSCs). *Applied Physics A* 122, 821.
- [5] Kovalenko, A., Rublev, P.O., Tcelykh, L.O., Goloveshkin, A.S., Lepnev, L.S., Burlov, A.S., Vashchenko, A.A., Marciniak, L., Magerramov, A.M., Shikhaliyev, N.G., Vatsadze, S.Z. & Utochnikova, V.V. (2019). Lanthanide complexes



Cover Page



with 2-(tosylamino)-benzylidene-N-(aryloyl)hydrazones: universal luminescent materials. *Chemistry of Materials* 31(3), 759-773.

[6] Liu, D., Zhou, Y.N., Zhao, J., Xu, Y., Shen, J. & Wu, M. (2017). An intensive green emitting terbium complex using a newly designed aromatic hyperbranched polyester as an efficient antenna ligand. *Journal of Materials Chemistry C* 5, 11620-11630.

[7] Yip, Y.W., Wen, H., Wong, W.T., Tanner, P.A. & Wong, K.L. (2012). Increased antenna effect of the lanthanide complexes by control of a number of terdentate N-donor pyridine ligands. *Inorganic Chemistry* 51(13), 7013-7015.

[8] Zhao, F. & Ma, D. (2017). Approaches to high performance white organic light-emitting diodes for general lighting. *Materials Chemistry Frontiers* 1, 1933-1950.

[9] Ugale, A., Kalyani, T.N. & Dhoble, S.J. (2018). *Lanthanide-Based Multifunctional Materials*, Elsevier, (USA) 59-97.

[10] Sivakumar, S. & Reddy, M.L.P. (2012). Bright green luminescent molecular terbium plastic materials derived from 3,5-bis(perfluorobenzyloxy)benzoate. *Journal of Materials Chemistry* 22, 10852-10859.

[11] Ajlouni, A.M., Taha, Z.A., Al-Hassan, K.A. & Anzeh, A.M.A. (2012). Synthesis, characterization, luminescence properties and antioxidant activity of Ln(III) complexes with a new aryl amide bridging ligand. *Journal of Luminescence* 132, 1357-1363.

[12] Khanagwal, J., Khatkar, S.P., Dhankhar, P., Bala, M., Kumar, R., Boora, P. & Taxak, V.B. (2020). Synthesis and photoluminescence analysis of europium(III) complexes with pyrazole acid and nitrogen containing auxiliary ligands. *Spectroscopy Letters* 53(8), 625-647.

[13] Gao, B., Zhang, D. & Don, T. (2015). Preparation and photoluminescence properties of polymer-rare-earth complexes composed of bidentate schiff-base-ligand-functionalized polysulfone and Eu(III) Ion. *Journal of Physical Chemistry C* 119(29), 16403-16413.

[14] Wang, X.L. & Yan, B. (2012). Photofunctional binary and ternary $\text{Eu}^{3+}/\text{Tb}^{3+}$ hybrid materials with copolymer linkage methacrylic acid-vinyltrimethoxysilane and 1,10-phenanthroline. *Colloids Surface A* 399, 18-24.

[15] Zhang, X., Zhang, W., Li, G., Xin, Z., Li, S., Guan, P. & Liu, Y. (2019). Preparation of a novel graphene oxide/rare-earth complexes hybrid material and its luminescent film. *Optical Materials* 98, 109425.

[16] Deopa, N. & Rao, A.S., (2017). Spectroscopic studies of Sm^{3+} ions activated lithium lead alumino borate glasses for visible luminescent device applications. *Optical Materials* 72, 31-39.

[17] Lou, Z. & Hao, J. (2004). Cathodoluminescence of rare-earth-doped zinc aluminate films. *Thin Solid Films* 450, 334-340.

[18] Wei, C., Xu, D., Yang, Z., Li, J., Chen, X., Li, X. & Sun, J. (2019). Synthesis and photoluminescence properties of Eu^{3+} -activated double perovskite Ba_2YTbO_6 red phosphor. *Journal of Electronic Materials* 48(8), 5048-5054.

[19] Teotonio, E.E.S., Espinola, J.G.P., Brito, H.F., Malta, O.L., Oliveira, S.F., de Faria, D.L.A. & Izumi, C.M.S. (2002). Influence of the N-[methylpyridyl]acetamide ligands on the photoluminescent properties of Eu(III)-perchlorate complexes. *Polyhedron* 21, 1837-1844.

[20] Sheng, K., Yan, B., Qiao, X.F. & Guo, L. (2010). Rare earth (Eu/Tb)/phthalic acid functionalized inorganic Si-O/organic polymeric hybrids: Chemically bonded fabrication and photophysical property. *Journal of Photochemistry & Photobiology A Chemistry* 210, 36-43.

[21] Rajamouli, B., Viswanathan, C.S.D., Giri, S., Jayasankar, C.K. & Sivakumar, V. (2017). Carbazole functionalized new bipolar ligand for monochromatic red light-emitting Europium (III) complex: combined experimental and theoretical study. *New Journal of Chemistry* 41(8), 3112-3123.

[22] Park, S.J., Kim, J.Y., Yim, J.H., Kim, N.Y., Lee, C.H., Yang, S.J., Yang, H.K. (2018). The effective fingerprint detection application using $\text{Gd}_2\text{Tb}_2\text{O}_7:\text{Eu}^{3+}$ nanophosphors. *Journal of Alloys Compounds*. 741, 246-255.

[23] Khanagwal, J., Kumar, R., Devi, R., Bala, M., Sehrawat, P., Khatkar, S.P. & Taxak, V.B. (2020). Photoluminescence performance of green light emitting terbium (III) complexes with β -hydroxy ketone and nitrogen donor ancillary ligands. *Luminescence* 36(3), 742-754.



Cover Page



-
- [24] Steemers, F.J., Verboom, W., Reinhoudt, D.N., VanderTol, E.B. & Verhoeven, J.W. (1995). New sensitizer-modified calix[4]arenes enabling near-UV excitation of complexed luminescent lanthanide ions. **Journal of American Chemical Society** 117, 9408-9414.
- [25] Latva, M., Takalo, H., Mikkala, V.M., Matachescu, C., RodriguezUbis, J.C. & Kankare, J. (1997). Correlation between the lowest triplet state energy level of the ligand and lanthanide(III) luminescence quantum yield. *Journal of Luminescence* 75, 149-169.